ACS Sustainable Chemistry & Engineering

Research Article

pubs.acs.org/journal/ascecg

Brønsted Acidic Polymer Nanotubes with Tunable Wettability toward Efficient Conversion of One-Pot Cellulose to 5-Hydroxymethylfurfural

Yunlei Zhang, Jianming Pan,* Yating Shen, Weidong Shi,* Chunbo Liu, and Longbao Yu

School of Chemistry and Chemical Engineering, Jiangsu University, Xuefu Road 301, Zhenjiang 212013, People's Republic of China

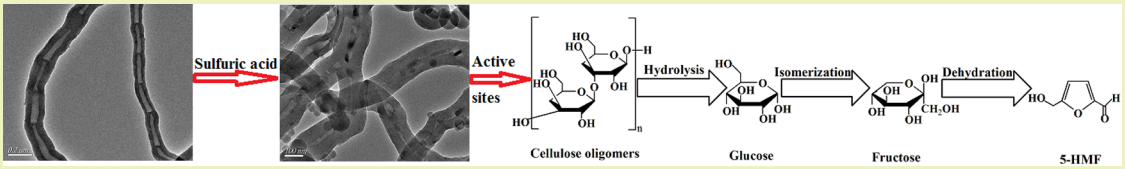

ABSTRACT: Employing renewable and widely available feedstock of cellulose as a raw material for 5-hydroxymethylfurfural (HMF) production opens up the possibility of sustainable biorefinery schemes that do not compete with the food supply. In this work, novel and efficient Brønsted acidic polymer nanotubes were successfully prepared by chemical conjugating grafting $-SO_3H$ groups onto the surface of polydivinylbenzene (PDVB) nanotubes, which were derived from cationic polymerization of divinylbenzene. By simply adjusting the grafting amounts of hydrophilic $-SO_3H$ groups, catalysts with varied hydrophobic and hydrophilic surface wettability (i.e., catalyst-110° and catalyst-10°) could be obtained. It was demonstrated that as-prepared catalyst-10° possessed the higher strong (143 μmol g^{-1}), very strong (614 μmol g^{-1}), and total acidity (786 μmol g^{-1}) than those of catalyst-110°. Besides, the catalytic performance of the synthesized catalyst-110° and catalyst-10° were investigated and compared for the conversion of cellulose to HMF in an ionic liquid (i.e., 1-ethyl-3-methyl-imidazolium chloride, [EMIM]-Cl) system. Particularly, catalyst-110° exhibited the highest HMF yield of 34.6% on a molar basis, which was comparable with that of catalyst-10° (i.e., 37.1%), indicating that its hydrophobic nature was beneficial for decreasing side-reaction of HMF which tend to convert to some other byproducts during the very one-pot reaction. Furthermore, both catalysts can be easily recovered and reused for at least four times without significant loss of their catalytic activities. This work was the continue efforts for fabrication and application solid catalyst for excellent conversion of one-pot cellulose to HMF.

KEYWORDS: *Sustainable chemistry, Cellulose, 5-Hydroxymethylfurfural, Brønsted acid, Polymer nanotubes, Adjusted wettability*

INTRODUCTION

With increasing consumption and depletion of traditional fossil fuel reserves, exploring renewable resources are essential for the sustainable development of chemicals and fuels. As the only sustainable source of organic carbon and primary-energy carrier, abundant biomass evolved as the most promising alternative to supply valuable intermediates to the chemical industry in a carbon-neutral way.[1] Among these priority chemicals, the versatile and top value-added 5-hydroxymethylfurfural (HMF) has received significant attention as a platform chemical for the production of a broad range of chemicals and liquid transportation fuels.[2] During the past few decades, the transformation of glucose and fructose for the production of HMF has been widely studied.[3] Although moderate to high HMF yields from glucose or fructose have been achieved, sustainable and economically viable routes for HMF production in scalable quantities arose serious challenges due to the high-cost of glucose and fructose. Moreover, adopting these types of edible sugars as raw materials for HMF production may compete with the food supply.

Accordingly, employing the most abundant organic compound of inedible cellulose for the production of HMF would be preferable. The utilization of cellulose, which is abundant among lignocellulosic materials such as wood, straw, grass, municipal solid waste, and crop residues, does not compete with the food supply.[4] It is clearly illustrated in Scheme 1 that the direct transformation of cellulose into HMF involves multiple steps, namely, hydrolysis, isomerization, and final dehydration to HMF. Rapid progress in the development of efficient catalysts for the conversion of cellulose has been witnessed over the past years, among which several homogeneous catalysts systems, including Brønsted and Lewis acid catalysts, have been reported effective for the bulk conversion of cellulose into HMF.[5,6] Although valuable results were obtained during the catalytic tests, the large scale production of HMF via cellulose degradation can hardly be commercially implemented due to several challenges met concerning corrosion, energy demand, and catalyst recovery.[7] To overcome these issues, several heterogeneous acidic mesoporous materials such as mesoporous silica nanopraticles,[8] different types of nanoporous zeolites derived from recrystallization[9] or the surfactants-assisted modification process,[10,11] and mesoporous zirconia nanoparticles[12] have been adopted as solid catalysts for the one-pot cellulose-to-HMF conversion due

Received: December 25, 2014
Revised: March 5, 2015
Published: March 24, 2015

DOI: 10.1021/sc5008412
ACS Sustainable Chem. Eng. 2015, 3, 871−879

Scheme 1. Cellulose Extracted Source and Cellulose-to-HMF Process

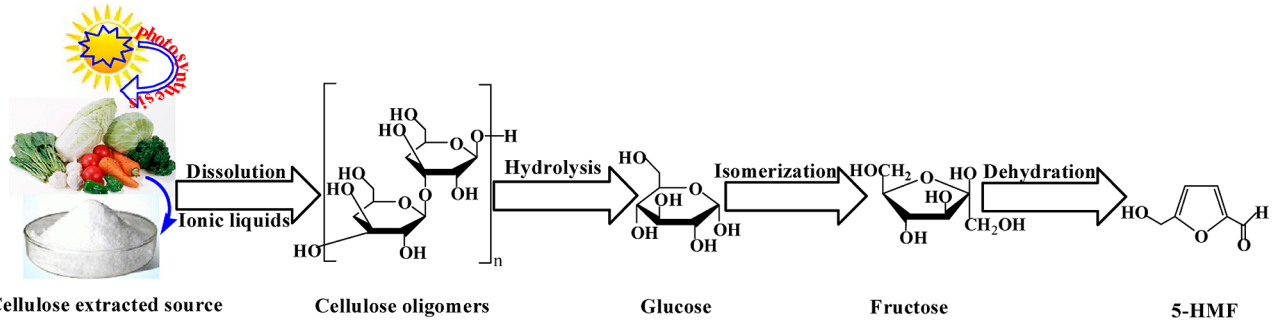

to their merits of environmentally friendly, good recyclability, and reductive corrosion.[13]

As the existence of acidic sites is necessary for the cellulose hydrolysis and monosaccharide dehydration processes, catalyst acidity is determined as a key factor influencing the corresponding catalytic performance.[5] Nevertheless, in the presence of an acid catalyst, HMF was prone to recombination with sugars or oligosaccharides via aldol condensation in the catalytic systems, resulting in polymers with undefined structures and stoichiometry called humins, which had a negative role in HMF yields.[14] Recently, many effective ways have been adopted to inhibit the side-reaction of HMF to some other byproducts. For instance, Dumesic and co-workers successfully developed a two-phase reactor system to continuously extract the HMF product from the aqueous phase, leading to high HMF yield.[15] In addition, the conclusion can be drawn that the side-reaction of HMF hydration occurred on acidic sites with water molecules. Therefore, by adjusting the catalyst surface wettability, a catalyst with strong acid strength and hydrophobicity was synthesized by Xiao's group.[16] As a consequence, HMF can be effectively protected by isolating the acidic sites from water molecules in their work.

Recently, nanomaterials with tubular structures have gained much attention in the catalytic field owing to their practical hollow tubular structures that can improve the accessibility of active sites with reactants.[17] In our previous work, halloysite nanotubes (HNTs) were employed as a catalysts supporter to synthesize multifunctional catalysts and tested for HMF production from cellulose.[18,19] The obtained catalysts showed advantageous catalytic performance and recyclability in the catalytic systems. In particular, the versatile organic nanotubes have attracted a surge of interest in biological systems, such as absorbents for organic chemicals and so on.[20] Therefore, many methods have been proposed including self-assembly, template synthesis, and electrospinning to synthesize organic nanotubes.[21,22] Compared with tedious and time-consuming methods for polymer nanotubes synthesis mentioned above, another versatile and simple approach of cationic polymerization would be preferable for efficient large scale synthesis of polymer nanotubes because the polymerization is extremely fast at room temperature, which can finish within minutes.[23] Based on fast cationic polymerization, several polymer nanotubes have been synthesized in large scale and used as absorbents for organic solvents[24] and heavy metal ions.[25] To the best of our knowledge, there are few reports about employing cationic polymerization to synthesize polymer nanotubes used in the biomass transformation field.

Enlightened by the information mentioned above, a cationic polymerization method and subsequent sulfonating process were combined to synthesize Brønsted acidic polymer nanotubes catalysts for one-pot cellulose-to-HMF conversion based on ionic liquids (ILs) system. First, immiscible initiator nanodroplets of boron trifluoride etherate (BFEE) was adopted to make the cationic polymerization of divinylbenzene (DVB) occur in cyclohexane solution. Second, by simply adjusting the grafting amounts of hydrophilic sulfo groups ($-SO_3H$) onto the surface of obtained superhydrophobic polydivinylbenzene (PDVB) nanotubes through a sulfonating process, hydrophobic and hydrophilic polymeric solid catalysts were successfully synthesized. The morphology and various properties of catalysts were characterized, and the catalytic performance in one-pot cellulose conversion was discussed in detail. Moreover, the regeneration performance of the catalysts was also studied.

EXPERIMENTAL SECTION

Materials. Cellulose (powder, ca. 50 μm), pure HMF, BFEE, 1-ethyl-3-methyl-imidazolium chloride ([EMIM]-Cl), and DVB were purchased from Aladdin Reagent Co., Ltd. (Shanghai, China) and used as received. Sulfuric acid (H_2SO_4), ethanol, HPLC-grade methanol, and cyclohexane were obtained from Sinopharm Chemical Reagent Co., Ltd. (Shanghai, China). All other chemicals were supplied by local suppliers and used without further purification.

Catalysts Preparation. PDVB nanotubes were synthesized as reported in previous literature with a slight modification.[26] To a 500 mL round-bottomed flask containing 150 mL of cyclohexane and 0.5−2.0 wt % of monomer DVB stirred at room temperature was initiated cationic polymerization after the immiscible initiator of BFEE (0.12 wt %) was slowly added, followed by stirring of the mixture at room temperature for about 120 s. To stop growth of the nanotubes, 10 mL of ethanol was added to terminate the polymerization. The samples were filtered and washed with ethanol to remove the residual initiator and monomer. After residual ethanol was evaporated, the nanotubes powder was obtained. In this work, Brønsted acidic polymer nanotubes catalysts with different surface wettabilities were obtained by varying the sulfonation conditions to introduce varied amounts of hydrophilic $-SO_3H$ onto the surface of obtained superhydrophobic PDVB nanotubes. The final catalysts were denoted as catalyst-A, where A stood for the contact angle (CA) of catalysts for water. In a typical run, the as-prepared PDVB nanotube powder (0.2 g) was immersed in concentrated sulfuric acid (10 mL) under stirring at 30 °C for 4 h. In a contrast experiment, the sulfonation process was taken out at 70 °C for 12 h and other parameters were same as previous. After the products were repeatedly washed with ethanol and water, sulfonated PDVB nanotubes were obtained after filtration.

Catalysts Characterization. Morphology of the products were analyzed via field emission scanning electron microscopy (SEM), which was carried out with an electron microscope equipped with a field emission electron gun and energy dispersive spectrometry (EDS). The morphology of the nanotubes were characterized by transmission scanning electron microscopy (TEM). Thermogravimetric analysis (TGA) of samples was performed for powder samples (about 10 mg) using a Diamond TGA/differential thermal analysis (DTA) instru-

DOI: 10.1021/sc5008412
ACS Sustainable Chem. Eng. 2015, 3, 871−879

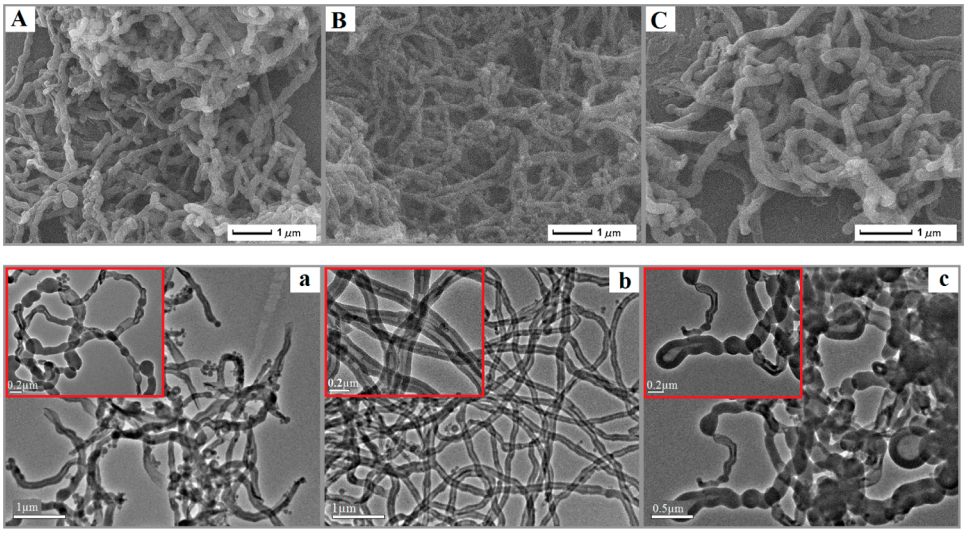

Figure 1. (A–C) SEM images of PDVB nanotubes prepared with 0.5, 1.0, and 2.0 wt % of monomer DVB, respectively. (a–c) Corresponding TEM of PDVB nanotubes.

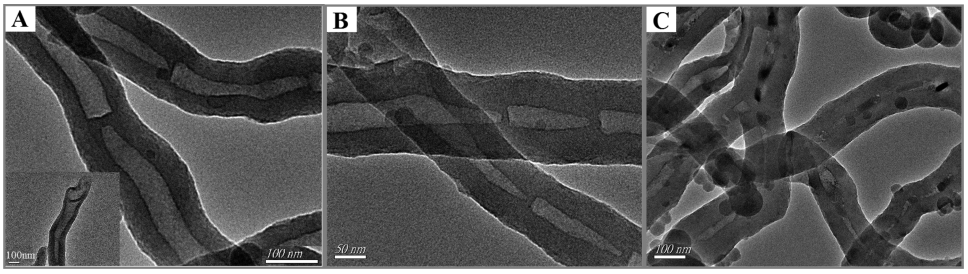

Figure 2. TEM images of PDVB nanotubes prepared with 1.0 wt % of monomer DVB (A), sulfonated nanotubes obtained with sulfonation temperature at 30 (B) and 70 °C (C).

ments under a nitrogen atmosphere up to 800 °C with a heating rate of 5.0 °C/min. X-ray photoelectron spectroscopy (XPS) spectra were performed on a Thermo ESCALAB 250 with Al Kα radition at y = 901 for the X-ray sources, and the binding energies were calibrated using the C 1s peak at 284.9 eV. Fourier transform infrared (FT-IR) spectra of the samples were tested on Nicolet NEXUS-470 FTIR apparatus (U.S.A.), which was recorded using KBr pellets for solid samples. CA of catalysts measurement was performed on optical contact angle measuring device. The concentration of sulfur in final products was measured by inductively coupled plasma-atomic emission spectrometry (ICP-AES) analysis. The acidic feature was determined by means of NH_3 temperature-programmed desorption (NH_3-TPD) using a TP 5000-II multiple adsorption apparatus (Tianjin Xianquan Corporation of Scientific Instruments, China). Typically, approximately 100 mg of catalyst was pretreated in a helium atmosphere at 40 °C for 1.0 h. When the mass baseline was stable, the helium flow was stopped, and NH_3 was introduced until adsorption of the samples was saturated. Then, the purging with the helium was performed to remove residual NH_3 from the surface of the samples. Subsequently, the samples were heated from 40 to 800 °C under flowing helium at a rate of 10 °C/min for NH_3 desorption. The acidity of catalysts was measured by the amounts of desorbed NH_3, which were calculated based on eq 1:

$$Q = Q_N \times \frac{A}{A_T} \times 100\% \quad (1)$$

where Q_N (μmol/g) is the total amount of desorbed NH_3, A is the corresponding deconvolution area of one NH_3-desorption peak, A_T is the total deconvolution area of all the NH_3-desorption peaks, and Q (μmol/g) is the amount of desorbed NH_3 corresponding to the TPD peak of relative area A.

Catalytic Evaluation and Analysis. Because of insoluble property in conventional solvents,[27] cellulose was pretreated with ILs of ([EMIM]-Cl) to destroy its rigid framework. All the cellulose dehydration reaction experiments were performed in 15 mL round-bottom flasks under magnetic stirring, unless otherwise mentioned. The cellulose conversion included two steps of pretreatment and catalytic reaction. In a typical experiment for pretreatment, cellulose (0.1 g) was added into 2.0 g of [EMIM]-Cl, and the whole mixture was heated at 120 °C and stirred at 800 r min^{-1} for 0.5 h, so as to dissolve cellulose. For the typical catalytic reaction step, the catalyst (30 mg) was added into the cellulose/[EMIM]-Cl solution while kept heating and stirring at 800 r min^{-1} at the optimized conditions. All reaction steps were repeated three times and the average yields of products were obtained.

The HMF was analyzed by a 1200 Agilent high performance liquid chromatography (HPLC) instrument equipped with an Agilent TC-C18(2) column (4.6 × 250 mm, 5.0 μm) and UV detector at 283 nm. During this process, the temperature of the column remained constantly at 25 °C, and the mobile phase was HPLC-grade methanol–water (7:3, v/v) at a flow rate of 0.7 mL min^{-1}, and 22.5 μL of each sample was also injected manually. The content of HMF was calculated based on the standard curve obtained with standard substances. And the HMF yield was defined as the molar ratio of moles of HMF in the obtained products and moles of initial cellulose, which was expressed in eq 2:

$$Y_{HMF}(\%) = \frac{\text{moles of HMF obtained}}{\text{moles of initial cellulose}} \times 100 \quad (2)$$

Recyclability of Catalysts. The recycling efficiency of the catalysts was determined for the dehydration of cellulose to HMF. After the reaction, the flask was cooled to room temperature, and the

DOI: 10.1021/sc5008412
ACS Sustainable Chem. Eng. 2015, 3, 871–879

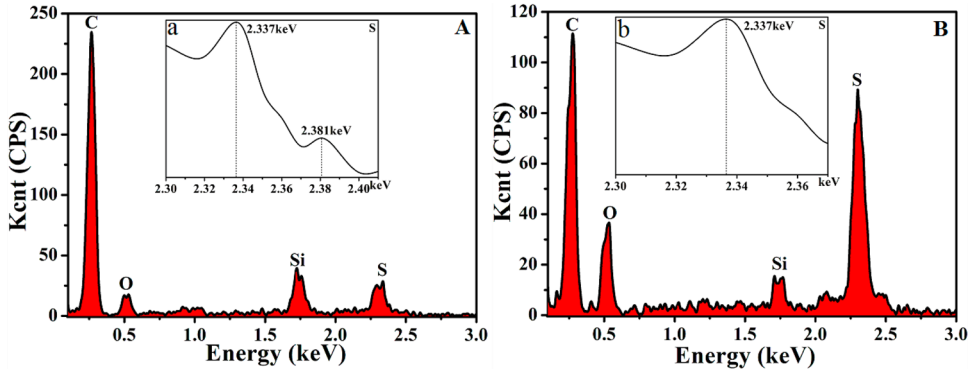

Figure 3. Energy dispersive spectrometry (EDS) of sulfonated nanotubes obtained with sulfonation temperatures at 30 and 70 °C, respectively.

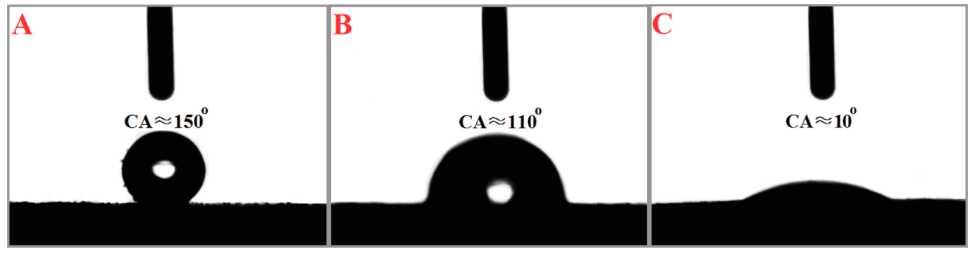

Figure 4. Contact angles of a water droplet on the surface of PDVB nanotubes (A), catalyst-110° (B), and catalyst-10° (C), respectively.

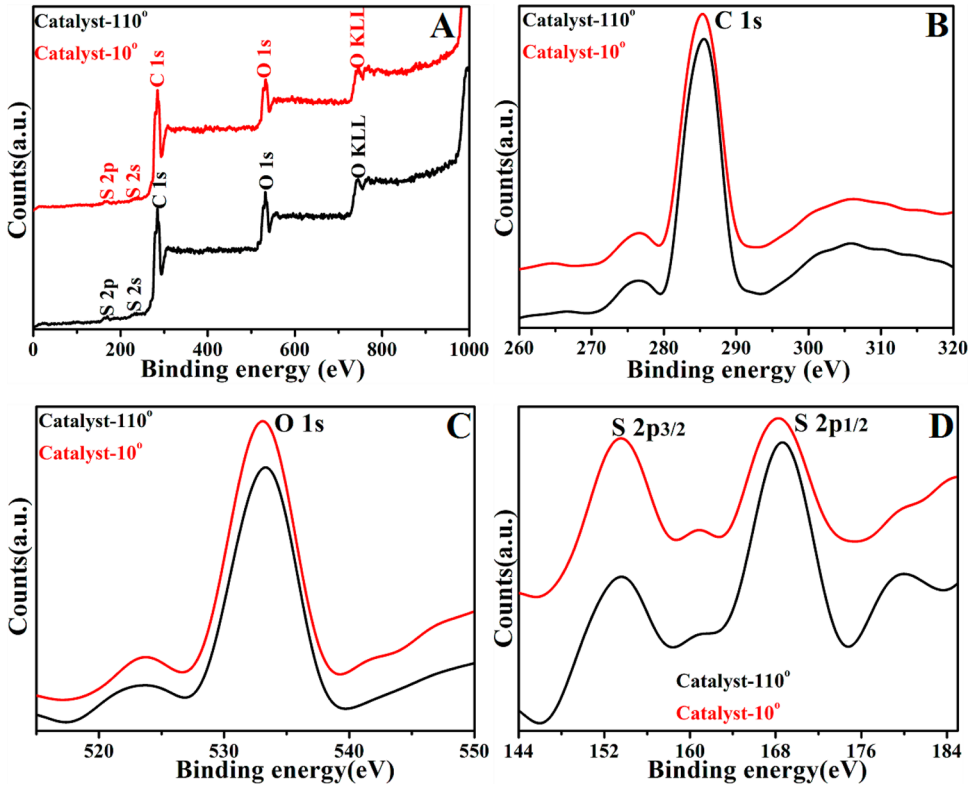

Figure 5. XPS spectrum of catalyst-110° and catalyst-10°.

catalysts were separated from the reaction mixture by filtration and centrifugation, washed 10 times with a mixture of deionized water and ethanol and dried at 80 °C for 24 h in a vacuum oven. Subsequently, the obtained recycling catalysts were reused for four consecutive cycles to produce HMF from cellulose at the reaction conditions that as same as the fresh experiments. The HMF yield was determined from each run.

RESULTS AND DISCUSSION

Physico-Chemical Properties of Catalysts. Figure 1A–C exhibits the SEM images of obtained PDVB nanotubes prepared from 0.5, 1.0, and 2.0 wt % of monomer DVB, respectively. And their relevant TEM observations are listed at below. At a relatively lower monomer concentration (i.e, 0.5 wt %), short nanotubes appeared (Figure 1A,a). As shown in

DOI: 10.1021/sc5008412
ACS Sustainable Chem. Eng. 2015, 3, 871–879

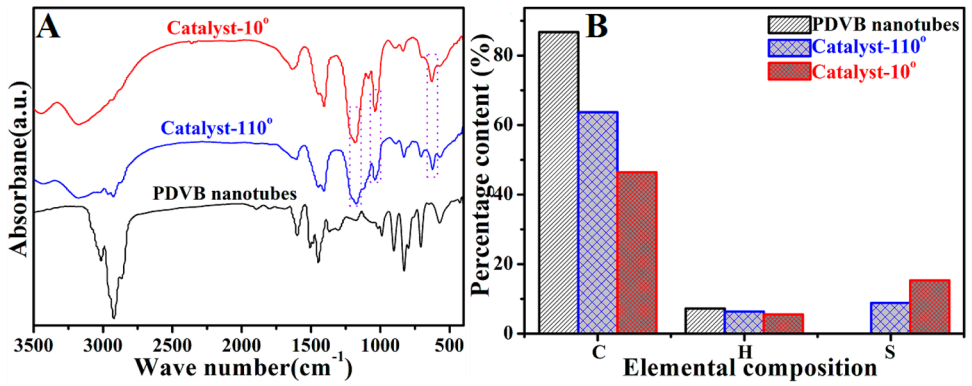

Figure 6. FT-IR (A) and elemental analysis (B) of PDVB nanotubes, catalyst-10° and catalyst-110°.

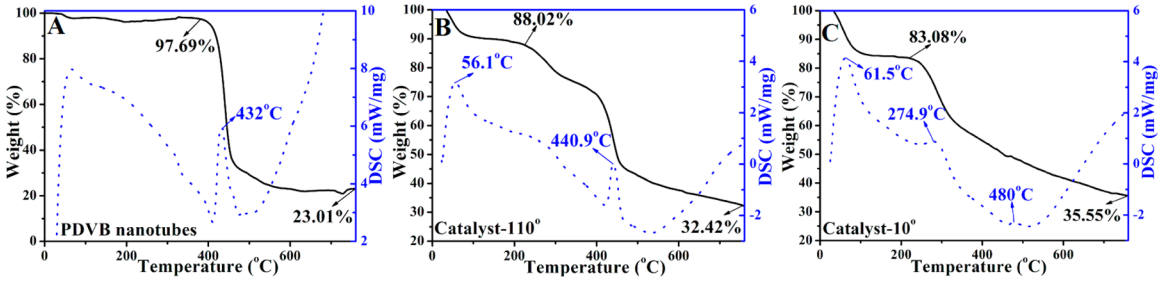

Figure 7. TG and DTG curves of PDVB nanotubes (A), catalyst-110° (B), and catalyst-10° (C).

Figure 1B,b, when the monomer concentration further increased to 1.0 wt %, a bamboo-like structure with a uniform diameter of 100 nm was preserved. It has been reported that bamboo-like nanotubes possessed enhanced strength owing to the mechanical support by the knots.[28] Gratifyingly, these polymer nanotubes can be synthesized in bulk within only 120 s. Interestingly, at higher monomer concentrations (2.0 wt %), however, shorter tadpole-like ones were achieved (Figure 1C,c), and tails of the tadpole-like nanotubes became thinner.

Figure 2 presents the TEM images of as-prepared primary PDVB nanotubes prepared with 1.0 wt % of monomer DVB (A), and sulfonated nanotubes obtained with sulfonation temperatures at 30 (B) and 70 °C (C) as described in the Experimental Section. It can be clearly seen that the structure of the nanotubes maintained well after the treatment with concentrated sulfuric acid, suggesting the enhanced mechanical strength of PDVB nanotubes. In addition, no obvious changes were observed either in its interior or exterior surface compared with sulfonated nanotubes obtained at 30 °C (B) and original PDVB nanotubes (A). However, a remarkable difference appeared in the interior surface, as shown in Figure 2C, that an obvious sulfonation shell could be observed. This was mainly caused by an increased amount of the $-SO_3H$ group grafting through the open ends, as listed in left bottom of Figure 2A. Additionally, the diameter of sulfonated nanotubes increased to 117 (B) and 150 nm (C), respectively.

EDS analysis equipped with SEM for sulfonated nanotubes obtained with sulfonation temperature at 30 (A) and 70 °C (B) are listed in Figure 3. Obviously, the existence of elements O and S peaks suggested the successful introduction of $-SO_3H$ onto the surface of PDVB nanotubes. Moreover, the S element in Figure 3a gave two peaks (2.337 and 2.381 keV), whereas only one peak (2.337 keV) could be observed in Figure 3b. Si peaks in both images were derived from the silicon slice used in SEM observation.

Figure 4A presents the water contact angle of the as-prepared PDVB nanotubes. Clearly, unmodified PDVB nanotubes gave the contact angle of nearly 150°, indicating its excellent water-repellent behavior. However, concentrated sulfuric acid treated PDVB nanotubes at 30 °C exhibited a relatively weakened hydrophobic property (Figure 4B) compared with the original ones due to the successful introduction of hydrophilic $-SO_3H$ groups onto the surface of PDVB nanotubes. Furthermore, hydrophilic catalyst was obtained when increased sulfonation temperature and more time were applied (contact angle was nearly 10° in Figure 4C), suggesting more hydrophilic $-SO_3H$ groups were grafted onto the surface of PDVB nanotubes. Generally, the different conditions of the sulfonation process not only resulted in varied catalyst surface wettabilities but their corresponding acidity, which will be discussed below in detail. Based on the different water contact angles, the final catalysts were renamed as catalyst-110° and catalyst-10°, respectively.

Figure 5 exhibits the XPS measurements of catalyst-110° and catalyst-10°, respectively. It can be clearly seen from Figure 5A that strong peaks of C 1s, O 1s, S 2p, and S 2s appeared both in catalyst-110° and catalyst-10°. Notably, the high-resolution C 1s spectrum in Figure 5B showed the signals at around 284.7 and 286.2 eV associated with C−C and C−S, which also demonstrated the successful introduction of sulfonic groups onto the surface of nanotubes. Another signal showed in high resolution XPS spectra at 533.1 eV was related to O 1s (Figure 5C). In Figure 5D, the S 2p spectra consisting of two individual peaks at 153.6 and 168.2 eV can be attributed to S $2p_{3/2}$ and S $2p_{1/2}$ binding energies. Because the binding energy of S 2p was sensitive to the acidic strength,[29] acid strength of the sulfonic groups in catalyst-110° and catalyst-10° could be proved. These results confirmed that Brønsted acidic polymer nanotubes catalysts have been successfully synthesized by our group.

FT-IR (A) and elemental analysis (B) of as-prepared nanotubes and final catalysts are presented in Figure 6.

DOI: 10.1021/sc5008412
ACS Sustainable Chem. Eng. 2015, 3, 871−879

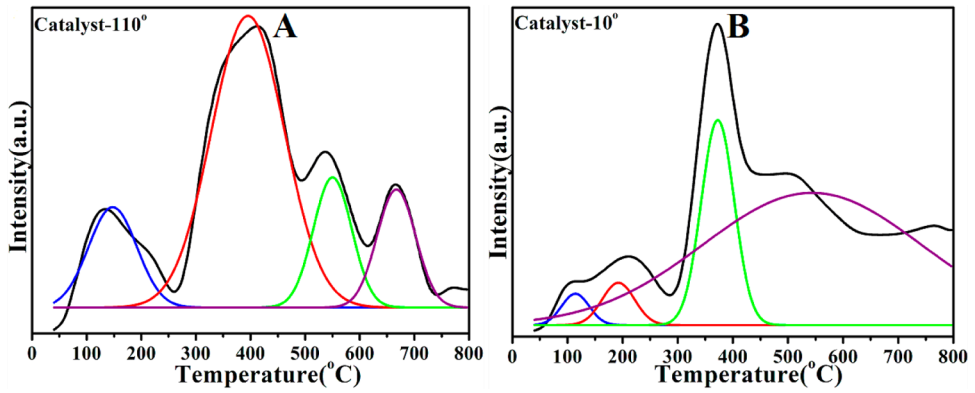

Figure 8. NH_3-TPD curves of catalyst-110° (A) and catalyst-10° (B).

Table 1. Acid Strength of Catalyst-110° and Catalyst-10°

	acid strength feature				
catalysts	weak (μmol g^{-1})	medium (μmol g^{-1})	strong (μmol g^{-1})	very strong (μmol g^{-1})	total (μmol g^{-1})
catalyst-110°	50		222	100	372
catalyst-10°	29		143	614	786

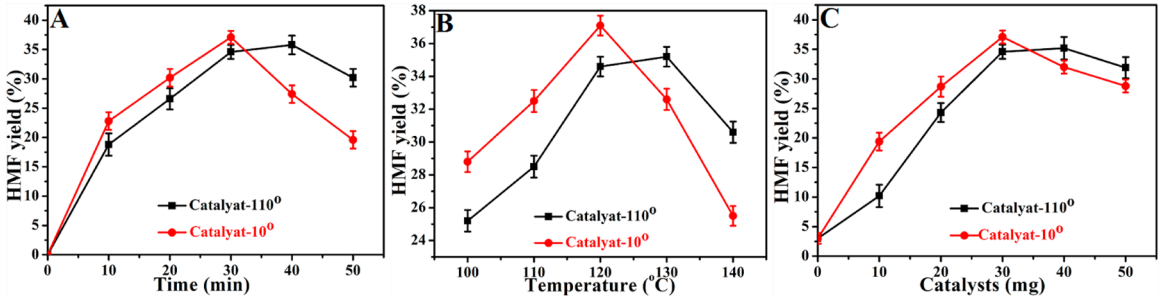

Figure 9. Effects of reaction time (A), temperature (B), and catalysts loading (C) on HMF yields from cellulose.

Compared with unmodified PDVB nanotubes, new peaks around ~670 and ~1073 cm^{-1} associated with the C—S bond, and ~1182 cm^{-1} associated with the O═S═O stretching vibration were clearly observed both in catalyst-110° and catalyst-10° (Figure 6A), indicating the presence of sulfonic group.[30] This further confirmed that the organic polymer nanotubes and sulfonic groups were successfully combined, which were in good agreement with the results from XPS analysis. Elemental analysis revealed that the percentage of carbon components gradually decreased from 86.62% to 63.83% (catalyst-110°) and 46.50% (catalyst-10°), respectively, while the percentage of sulfur components gradually increased and the highest value of 15.21% with catalyst-10° was achieved. This also proved that more $-SO_3H$ groups were grafted onto the surface of catalyst-10°, which was consistent with the results obtained from CA analysis.

Figure 7 shows the TG and DSC curves of PDVB nanotubes and final catalysts. TG analysis of all samples displayed mass loss, and corresponding DSC curves pointed out the endothermic or exothermic reactions according to peak temperature. As shown in Figure 7A, PDVB nanotubes cannot be easily decomposed within the initial temperature range (<400 °C), and the endothermic peak for PDVB nanotubes was attributed to the decomposition of outer shell grafting polymer (around 432.0 °C), as observed in Figure 7A. The significant weight loss of PDVB nanotubes (76.99%) occurred when the temperature increased to 800 °C. Beyond 800 °C, the remaining mass for PDVB nanotubes may be attributed to the residual carbonized polymers. Interestingly, catalyst-110° and catalyst-10° showed obvious weight loss within temperature range from 25 to 500 °C (Figure 7B,C), owing to the loss of structure water. Moreover, catalyst-10° exhibited even higher weight loss than catalyst-110° due to its hydrophilic nature. With the temperature increased to 800 °C, weight losses resulted from decomposition of sulfonic groups and network of 65.36% and 58.23% of were tested for catalyst-110° and catalyst-10°, respectively. The TG curves of catalyst-110° and catalyst-10° with the same trend further indicated that they probably possessed similar morphological structure and size distribution. In DSC curves, the endothermic peaks for catalyst-110° (around 56.10, 440.9 °C), catalyst-10° (around 61.50, 279.4 °C), and exothermic peak for catalyst-10° (509.0 °C) were also observed, which could be assigned to the decomposition of sulfonic groups and PDVB network.

The quantification of the catalysts acid density was evaluated by the NH_3-TPD method. Among the desorbed NH_3 molecules, those appearing at ≤150 °C should correspond to the physically adsorbed NH_3, and other desorbed NH_3 molecules at the higher temperatures were attributed to acid site bound NH_3.[31] The acid sites could be denoted as weak, medium, strong, and very strong at desorption temperatures of 150−250, 250−350, 350−500, and >500 °C, respectively.[32] Each of these desorption peaks in Figure 8 was integrated to measure the corresponding acid density as described in the

DOI: 10.1021/sc5008412
ACS Sustainable Chem. Eng. 2015, 3, 871−879

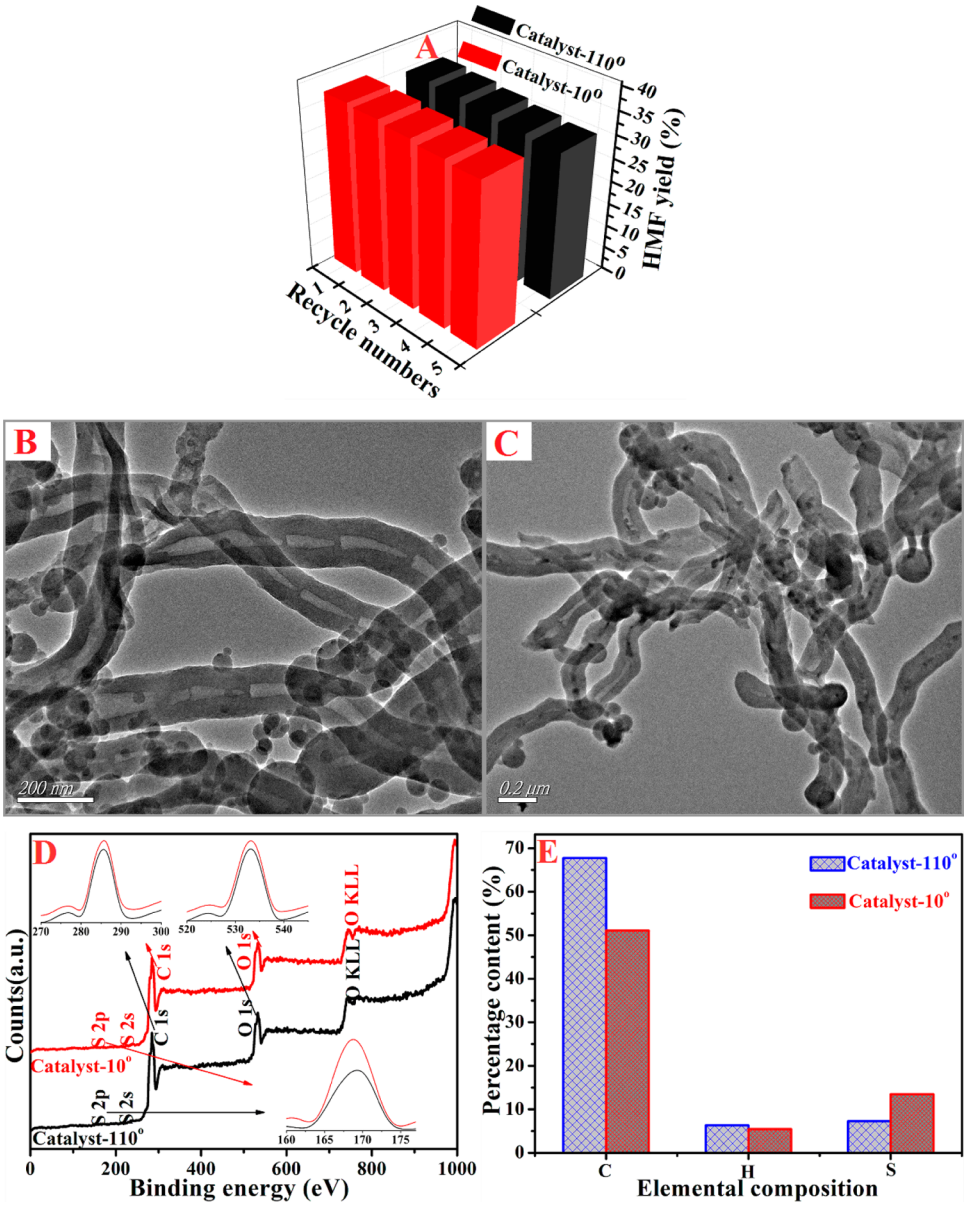

Figure 10. Recyclability of catalyst-110° and catalyst-10° in conversion of cellulose-to-HMF (A), SEM images of reused catalyst-110° and catalyst-10° after five times (B, C), XPS spectrum of catalyst-110° and catalyst-10° after regeneration (D), and elemental analysis of reused catalyst-110° and catalyst-10° after five times (E).

Experiment Section. Table 1 shows the corresponding acid strength for catalyst-110° and catalyst-10° in detail. Obviously, catalyst-10° possessed the relatively higher strong (143 μmol g^{-1}), very strong (614 μmol g^{-1}), and total acidity (786 μmol g^{-1}) than those of catalyst-110°.

Performance of Catalysts in Cellulose-to-HMF Conversion. The catalytic performances of catalyst-110° and catalyst-10° were evaluated by HMF yields from cellulose in ILs systems. To obtain the optimum conditions for cellulose conversion, varied reaction time, temperature, and catalyst dosage were studied in the reactors.

First, the effect of reaction time ranging from 10 to 50 min on HMF yields was investigated, while keeping the reaction temperature and catalysts dosage constant at 120 °C and 30 mg, respectively. As shown in Figure 9A, HMF yields gradually increased as the reaction time prolonged during the first 30 min both for catalyst-110° and catalyst-10°. The color of the reaction mixture was pale yellow, which is a clear indication that a significant amount of black humin oligomer[33] did not form under these conditions. However, a further prolonged reaction time to 50 min resulted in decreased HMF yields. It has been previously proved that an increase of the reaction temperature and time may result in the formation of some undesired byproducts such as soluble polymers and insoluble humins.[34] Although these undesired byproducts were difficult to indentify through present techniques, the generation of these byproducts could be confirmed through the color changes of the reaction mixture, which was in consistence with the results from Wang's work.[35] Furthermore, it can be clearly seen that highest HMF yields at 34.6% and 37.1% were obtained at 120 °C and 30 min with catalyst-110° and catalyst-10°, respectively. Therefore, subsequent experiments were performed over 30 min.

Second, the effect of temperature on HMF yields was studied by performing cellulose conversion at elevated temperatures

DOI: 10.1021/sc5008412
ACS Sustainable Chem. Eng. 2015, 3, 871−879

from 100 to 140 °C. Under constant reaction conditions of 100 mg of cellulose, 30 mg of catalyst, and 30 min reaction time, HMF yields catalyzed by catalyst-110° increased from 25.2% to 34.6% significantly as the temperature increased from 100 to 120 °C (Figure 9B). And HMF yields were also improved from 28.8% to 37.1% with catalyst-10°. Nevertheless, further increasing the temperature to 140 °C resulted in a dramatic decrease of HMF yields with both catalyst-110° and catalyst-10°. It has been said that HMF was prone to recombination with sugars or oligosaccharides via aldol condensation, resulting in polymers with undefined structures and stoichiometry called humins when the temperature was increased and closed to the melting point of monosaccharides.[36]

Finally, the conversion of cellulose to HMF was studied at various catalysts loadings to optimize the reaction conditions and maximize the HMF yields. Catalysts amounts were varied from 10 to 50 mg, while the other reaction parameters were constant: cellulose = 100 mg, T = 120 °C, t = 30 min. As shown in Figure 9C, HMF yields dramatically increased from 3% to 34.6% with catalyst-110°, while that increased to 37.1% with catalyst-110° upon increasing the catalysts loadings from 0 to 30 mg. However, further increase in catalyst loadings from 30 to 40 mg showed a minimal increase in the HMF yield from 34.6% to 35.2% with catalyst-110°, while the catalyst-10° showed a contradictory decreasing trend. Moreover, both catalyst-110° and catalyst-10° exhibited decrease trends of HMF yield as the catalyst loadings increased to 50 mg. According to various pioneer reports, acid catalysts were active in the direct hydrolysis of cellulose to glucose, HMF and other soluble byproducts.[28] However, overused catalysts were also beneficial for accelerating the side-reaction to produce more byproducts. This suggested that an optimized HMF yields can be achieved by using 30 mg of catalysts for 100 mg of cellulose substrate. Therefore, the optimized conditions for catalyst-110° and catalyst-10° were both 30 mg of catalysts, 30 min of reaction time, and 120 °C of reaction temperature. And under the optimized conditions, catalyst-110° and catalyst-10° enable maximum yields of HMF at 34.6% and 37.1%, respectively.

In the literature, it has been reported that catalyst acidity played a key role in improving HMF yields in biomass conversion.[5,6] And in our previous work, the existence of strong acidic active sites in catalysts showed advantageous property in enhancing catalysts performance.[19] In this work, although catalyst-10° possessed higher total acidity and more strong acidic active sites than those of catalyst-110°, HMF yields catalyzed by the catalysts were identified almost the same with each other, indicating that hydrophobic property was also beneficial for isolating product of HMF from water molecules and thus decrease the side-reaction of HMF to some other byproducts.

Recyclability of Catalysts. To make a further evaluation of the catalysts recyclability, catalyst-110° and catalyst-10° were selected to study the reusability in the cellulose-to-HMF conversion over four cycles. As shown in Figure 10A, the HMF yields remained at around 31.8% and 35.0% until the fourth run from cellulose with catalyst-110° and catalyst-10°, which were as comparable as that of fresh catalysts, respectively. No significant losses of HMF yield were observed until the fourth run, which means that the immobilized functional group of $-SO_3H$ did not largely leach during the repeated process. SEM images of reused catalyst-110° and catalyst-10° after five times listed in Figure 10B,C revealed that the catalysts' bamboo-like structure was well maintained during the catalytic process. The superior recyclability of catalyst-110° and catalyst-10° was resulted from their superior thermal stability of both acidic sites and polymer network, which were very important for their widely practical applications. These results, to some extent, suggested that the heterogeneous catalysts had the great potential to be effectively separated and reused for the dehydration reaction.

To further confirm the structural property of recycled catalysts, XPS spectra of fourth repeated used catalyst-110° and catalyst-10° are exhibited in Figure 10D. When compared with the XPS spectrum of the fresh catalysts shown in Figure 5A, strong peaks of C 1s, O 1s, S 2p, and S 2s can be observed, indicating the superior chemical stability of the as-prepared catalyst-110° and catalyst-10° during the repeated catalytic processes. Elemental analysis for the catalysts after the fifth run showed that S content decreased 1.597% with catalyst-110° and 1.860% with catalyst-10°, respectively (Figure 10E). Results of ICP-AES demonstrated that the concentration of sulfur in final products after fifth run were 0.06 mg/mL with catalyst-110° and 0.07 mg/mL with catalyst-10°, which were derived from the leaching of $-SO_3H$ groups.

CONCLUSIONS

In summary, based on the cationic polymerization method and subsequent sulfonating process, catalysts with hydrophobic and hydrophilic surface wettabilities (i.e., catalyst-110° and catalyst-10°) were successfully developed for the conversion of one-pot cellulose to HMF. Catalysts characterizations indicated that catalyst-10° possessed higher acid strength than catalyst-110°. However, the catalysts showed comparable catalytic activity for the dehydration of cellulose to HMF, which enables maximum yields of 37.1% with catalyst-10° and 34.6% with catalyst-110°, respectively, in the ILs solvent system under the optimized conditions. Catalyst-110° gave an only 2.5% lower HMF yield than catalyst-10° because its hydrophobic property was beneficial for isolating HMF from water molecules, thus decreasing the side-reaction of HMF to some other byproducts. Catalytic performance of the as-prepared catalysts proved that surface wettability of catalysts also acted a key role in determining catalytic effectiveness except for acid strength. This work was the continued efforts for making stable polymeric solid acid, and the results from this work could be valuable for future research toward development of new reactors, especially their wide application for biomass and bioenergy.

AUTHOR INFORMATION

Corresponding Authors

*Dr. Jianming Pan. E-mail: zhenjiangpjm@126.com. Tel.: +86 511 88830099. Fax: +86 511 88830099.

*Professor Weidong Shi. E-mail: jsdxswd@126.com. Tel.: +86 511 88791800. Fax: +86 511 88791800.

Notes

The authors declare no competing financial interest.

ACKNOWLEDGMENTS

This work was financially supported by the National Natural Science Foundation of China (No. 21107037, No. 21176107, and No. 21306013), Natural Science Foundation of Jiangsu Province (No. BK2011461, No. BK2011514), National Postdoctoral Science Foundation (No. 2013M530240), Postdoctoral Science Foundation funded Project of Jiangsu

DOI: 10.1021/sc5008412
ACS Sustainable Chem. Eng. 2015, 3, 871−879

Province (No. 1202002B), and Programs of Senior Talent Foundation of Jiangsu University (No. 12JDG090).

REFERENCES

(1) Tsilomelekis, G.; Josephson, T. R.; Nikolakis, V.; Caratzoulas, S. Origin of 5-hydroxymethylfurfural stability in water/dimethyl sulfoxide mixtures. *ChemSusChem* **2014**, *7*, 117−126.

(2) Dutta, S.; De, S.; Saha, B.; Alam, I. Advances in conversion of hemicellulosic biomass to furfural and upgrading to biofuels. *Catal. Sci. Technol.* **2012**, *2*, 2025−2036.

(3) van Putten, R.-J.; Soetedjo, J. N. M.; Pidko, E. A.; van der Waal, J. C.; Hensen, E. J. M.; Jong E, de; Heeres, H. J. Dehydration of different ketoses and aldoses to 5-hydroxymethylfurfural. *ChemSusChem* **2013**, *6*, 1681−1687.

(4) Rinaldi, R.; Meine, N.; vom Stein, J.; Palkovits, R.; Schüth, F. Which controls the depolymerization of cellulose in ionic liquids: The solid acid catalyst or cellulose? *ChemSuschem* **2010**, *3*, 266−276.

(5) Yang, Y.; Hu, C.; Abu-Omar, M. M. Conversion of carbohydrates and lignocellulosic biomass into 5-hydroxymethylfurfural using $AlCl_3 \cdot 6H_2O$ catalyst in a biphasic solvent system. *Green Chem.* **2012**, *14*, 509−513.

(6) Dutta, S.; De, S.; Alam, I.; Abu-Omar, M. M. Direct conversion of cellulose and lignocellulosic biomass into chemicals and biofuel with metal chloride catalysts. *J. Catal.* **2012**, *288*, 8−15.

(7) Rinaldi, R.; Schüth, F. Acid hydrolysis of cellulose as the entry point into biorefinery schemes. *ChemSusChem* **2009**, *2*, 1096−1107.

(8) Peng, W. H.; Lee, Y. Y.; Wu, C. N.; Wu, K. C. W. Acid-base bifunctionalized, large-pored mesoporous silica nanoparticles for cooperative catalysis of one-pot cellulose-to-HMF conversion. *J. Mater. Chem.* **2012**, *22*, 23181−23185.

(9) Torad, N. L.; Naito, M.; Tatami, J.; Endo, A.; Leo, S.-Y.; Ishihara, S.; Wu, K. C.-W.; Wakihara, T.; Yamauchi, Y. Highly crystallized nanometer-sized zeolite a with large Cs adsorption capability for the decontamination of water. *Chem.—Asian J.* **2014**, *9*, 759−763.

(10) Ivanova, I. I.; Knyazeva, E. E. Micro-mesoporous materials obtained by zeolite recrystallization: Synthesis, characterization and catalytic applications. *Chem. Soc. Rev.* **2013**, *42*, 3671−3688.

(11) Na, K.; Choi, M.; Ryoo, R. Recent advances in the synthesis of hierarchically nanoporous zeolites. *Microporous Mesoporous Mater.* **2013**, *166*, 3−19.

(12) Kuo, I.-J.; Suzuki, N.; Yamauchi, Y.; Wu, K. C.-W. Cellulose-to-HMF conversion using crystalline mesoporous titania and zirconia nanocatalysts in ionic liquid systems. *RSC Adv.* **2013**, *3*, 2028−2034.

(13) Stocker, M. Biofuels and biomass-to-liquid fuels in the biorefinery: Catalytic conversion of lignocellulosic biomass using porous materials. *Angew. Chem., Int. Ed.* **2008**, *47*, 9200−9211.

(14) Zhao, H. B.; Holladay, J. E.; Brown, H.; Zhang, Z. C. 5-Integrating enzymatic and acid catalysis to convert glucose into 5-hydroxymethylfurfural. *Science* **2007**, *316*, 1597−1600.

(15) Chheda, J. N.; Román-Leshkov, Y.; Dumesic, J. A. Production of 5-hydroxymethylfurfural and furfural by dehydration of biomass-derived mono- and poly-saccharides. *Green Chem.* **2007**, *9*, 342−350.

(16) Wang, L.; Wang, H.; Liu, F. J.; Zheng, A. M.; Zhang, J.; Sun, Q.; Lewis, J. P.; Zhu, L. F.; Meng, X. J.; Xiao, F. S. Selective catalytic production of 5-hydroxymethylfurfural from glucose by adjusting catalyst wettability. *ChemSusChem* **2014**, *7*, 402−406.

(17) Remskar, M.; Mrzel, A.; Virsek, M.; Jesih, A. Inorganic nanotubes as nanoreactors: The first MoS_2 nanopods. *Adv. Mater.* **2007**, *19*, 4276−4278.

(18) Zhang, Y. L.; Pan, J. M.; Gan, M. Y.; Ou, H. X.; Yan, Y. S.; Shi, W. D.; Yu, L. B. Acid-chromic chloride functionalized natural clay-particles for enhanced conversion of one-pot cellulose to 5-hydroxymethylfurfural in ionic liquids. *RSC Adv.* **2014**, *4*, 11664−11672.

(19) Zhang, Y. L.; Pan, J. M.; Yan, Y. S.; Shi, W. D.; Yu, L. B. Synthesis and evaluation of stable polymeric solid acid based on halloysite nanotubes for conversion of one-pot cellulose to 5-hydroxymethylfurfural. *RSC Adv.* **2014**, *4*, 23797−23806.

(20) Bong, D. T.; Clark, T. D.; Granja, J. R.; Ghadiri, M. R. Self-assembling organic nanotubes. *Angew. Chem., Int. Ed.* **2001**, *40*, 988−1011.

(21) Zhu, L.; Xu, Y.; Yuan, W.; Xi, J.; Huang, X.; Tang, X.; Zheng, S. One-pot synthesis of poly(cyclotriphosphazene-co-4,4′-sulfonyldiphenol) nanotubes via an in situ template approach. *Adv. Mater.* **2006**, *18*, 2997−3000.

(22) Greiner, A.; Wendorff, J. H. Electrospinning: A fascinating method for the preparation of ultrathin fibers. *Angew. Chem., Int. Ed.* **2007**, *46*, 5670−5703.

(23) Kesharwani, T.; Valenstein, J. S.; Trewyn, B. G.; Li, F.; Lin, V. S.-Y.; Larock, R. C. Synthesis of nanotubes via cationic polymerization of styrene and divinylbenzene. *Polym. Chem.* **2010**, *1*, 1427−1429.

(24) Zheng, F.; Baldwin, D. L.; Fifield, L. S.; Anheier, N. C.; Aardahl, C. L.; Grate, J. W. Single-walled carbon nanotube paper as a sorbent for organic vapor preconcentration. *Anal. Chem.* **2006**, *78*, 2442−2446.

(25) Sha, J.; Niu, J.; Ma, X.; Xu, J.; Zhang, X.; Yang, Q.; Yang, D. Hydrothermal synthesis of single-crystal $Ni(OH)_2$ nanorods in a carbon-coated anodic alumina film. *Adv. Mater.* **2002**, *14*, 1216−1219.

(26) Ni, W.; Liang, F. X.; Liu, J. G.; Qu, X. Z.; Zhang, C. L.; Li, J. L.; Wang, Q.; Yang, Z. Z. Polymer nanotubes toward gelating organic chemicals. *Chem. Commun.* **2011**, *47*, 4727−4729.

(27) Long, J. X.; Guo, B.; Li, X. H.; Jiang, Y. B.; Wang, F. R.; Tsang, S. C.; Wang, L. F.; Kai Man, K. Y. One step catalytic conversion of cellulose to sustainable chemicals utilizing cooperative ionic liquid pairs. *Green Chem.* **2011**, *13*, 2334−2338.

(28) Rodriguez, A. T.; Chen, M.; Chen, Z.; Brinker, C. J.; Fan, H. Nanoporous carbon nanotubes synthesized through confined hydrogen-bonding self-assembly. *J. Am. Chem. Soc.* **2006**, *128*, 9276−9277.

(29) Geim, A. K. Graphene: Status and prospects. *Science* **2009**, *324*, 1530−1534.

(30) Scaranto, J.; Charmet, A. P.; Giorgianni, S. IR spectroscopy and quantum-mechanical studies of the adsorption of CH_2CClF on TiO_2. *J. Phys. Chem. C* **2008**, *112*, 9443−9450.

(31) Ravindra Reddy, C.; Bhat, Y. S.; Nagendrappa, G.; Jai Prakash, B. S. Brønsted and Lewis acidity of modified montmorillonite clay catalysts determined by FT-IR spectroscopy. *Catal. Today* **2009**, *141*, 157−160.

(32) Liu, D.; Yuan, P.; Liu, H. M.; Cai, J. G.; Tan, D. Y.; He, H. P.; Zhu, J. X.; Chen, T. H. Quantitative characterization of the solid acidity of montmorillonite using combined FTIR and TPD based on the NH_3 adsorption system. *Appl. Clay Sci.* **2013**, *80*, 407−412.

(33) Dee, S. J.; Bell, A. T. A study of the acid-catalyzed hydrolysis of cellulose dissolved in ionic liquids and the factors influencing the dehydration of glucose and the formation of humins. *ChemSusChem* **2011**, *4*, 1166−1173.

(34) Flora, C.; Franck, R.; Catherine, P.; Amandine, C.; Emmanuelle, G.; Nadine, E. Cellulose hydrothermal conversion promoted by heterogeneous Brønsted and Lewis acids: Remarkable efficiency of solid Lewis acids to produce lactic acid. *Appl. Catal., B* **2011**, *105*, 171−181.

(35) Wang, J. J.; Xu, W. J.; Ren, J. W.; Liu, X. H.; Lu, G. Z.; Wang, Y. Q. Efficient catalytic conversion of fructose into hydroxymethylfurfural by a novel carbon-based solid acid. *Green Chem.* **2011**, *13*, 2678−2681.

(36) Sievers, C.; Musin, I.; Marzialetti, T.; Olarte, M. B. V.; Agrawal, P. K.; Jones, C. W. Acid-catalyzed conversion of sugars and furfurals in an ionic-liquid phase. *ChemSusChem* **2009**, *2*, 665−671.

DOI: 10.1021/sc5008412
ACS Sustainable Chem. Eng. 2015, 3, 871−879